Sensors and Actuators B 155 (2011) 67–74

Contents lists available at ScienceDirect

Sensors and Actuators B: Chemical

journal homepage: www.elsevier.com/locate/snb

Carbon nanotube based sensors for the detection of viruses

M. Bhattacharya[a,*], S. Hong[b], D. Lee[c], T. Cui[c], S.M. Goyal[d]

[a] Department of Bioproducts and Biosystems Engineering, University of Minnesota, United States
[b] Department of Civil Engineering, University of Minnesota, United States
[c] Department of Mechanical Engineering, University of Minnesota, United States
[d] Department of Veterinary Population Medicine, University of Minnesota, United States

ARTICLE INFO

Article history:
Received 12 July 2010
Received in revised form 12 October 2010
Accepted 15 November 2010
Available online 21 November 2010

Keywords:
Carbon nanotubes
Biosensors
Viruses

ABSTRACT

Carbon nanotube biosensors were assembled using a layer-by-layer (LBL) technique exploiting the chemical functionalization on nanotubes to tailor their interactions with viruses and antiviral antibodies. Gold electrodes were patterned in the form of resistors onto a Si/SiO_2 substrate, followed by stepwise LBL assembly to change the resistivity of the channel. Polyelectrolyte multilayer films were prepared by the sequential electrostatic adsorption of poly(diallyldimethylammonium chloride), poly(styrene sulfonate), and functionalized single-walled carbon nanotubes. Viral antibodies were successfully immobilized between the electrodes and the binding of antibodies to the surface was enhanced by coating with poly(L-lysine). An antigen specific to the immobilized antibody was captured on these devices. The coupled antibody–antigen complex changed the conductance of the device and this change was related to the antigen concentration. The two factors affecting the performance of the device were the number of layers and the channel length between the electrodes. We were able to detect conductance change for a viral antigen with a titer of 10^2 $TCID_{50}$/ml (50% tissue culture infective dose).

1. Introduction

Viruses are one of the main causes of disease in humans and animals. In addition, viruses can serve as agents for biologically related terrorism and warfare. Hence, rapid and accurate detection is important to prevent outbreaks and devastation. Current techniques of virus detection such as plaque assays, PCR-based testing, and microscopy require sample manipulation and are time consuming. The performance and sensitivity of biosensors can be improved by using nanomaterials for their construction [1]. Carbon nanotubes (CNTs) are emerging as building blocks of novel nanostructures and devices [2–5]. The large surface per unit mass (50–500 m^2/g) and excellent mechanical and electrical properties of CNTs make them particularly useful for electronic detection of biomolecules. The surface of the CNTs can be functionalized with appropriate chemical groups for attaching desired biomolecules (nucleic acids, enzymes, carbohydrates) or enhancing the solubility or biocompatibility of the tubes [6]. This concept can be exploited for sensor applications where the large surface area of an individual CNT or of a forest of CNTs can be used to immobilize antigen or antibody, which can then be used to capture their corresponding antibody or antigen, respectively. In this system, the analyte of interest binds specifically to the complementary biological recognition element immobilized on a suitable support medium. This immunoaffinity reaction can be detected by a change in the mechanical or electrical property of the CNTs. Electrochemical sensors can be based on potentiometry, amperometry, voltammetry, coulometry, AC conductivity or capacitance measurements [7,8].

Various nanoscale devices have been tested. Immunocapture on antibody coated chips has been used in direct visualization of viruses [9,10] using atomic force microscopy (AFM). For coxsackievirus, the limit of detection was 10^6–10^7 $TCID_{50}$/ml (50% tissue culture infective dose). Hepatitis C virus at fractional pM range was detected using single walled CNT field effect transistor devices using functionalized peptide nucleic acid [11]. Nanowires allow real time detection of single virus particle with high selectivity [12–14]. A single nanowire requires relatively high virus concentration (10^5 $TCID_{50}$/ml) to overcome the probability of the virus attaching to the sensor with small surface area. Sensitivity could be increased by increasing the number of nanowires [13]. The conductance change was proportional to the viral concentration and the system required no purification of the sample. Another advantage of these nanowire based devices is the detection of multiple analyte simultaneously in a single detection platform [12]. Ymeti et al. [15,16] used an integrated optical Young interferometer sensor for real-time direct detection of viruses. The detection limit of herpes simplex virus type 1 (HSV-1) was 850 virus particles/ml. There was a linear relation between the virus concentration and sensor signal. The device has several channels that can be used to monitor

* Corresponding author. Fax: +1 612-624-3005.
E-mail address: bhatt002@umn.edu (M. Bhattacharya).

0925-4005/$ – see front matter © 2010 Elsevier B.V. All rights reserved.
doi:10.1016/j.snb.2010.11.025

different analytes by coating the channel with different antibodies. The response time of these sensors can be as low as 5 min.

Detection of viruses in clinical and environmental samples using simple, rapid, and inexpensive methods is extremely important. Appropriate control measures can be implemented quickly if evidence of a virus is found. The reliability of treatment and control programs often depends on how rapidly viral contamination is detected. Methods for laboratory detection and identification of viruses are commonplace but methods that can be used in the field without requiring bulky equipment are scarce. Our proposed method will be helpful in overcoming some of the said problems. In this study, we explore how nanotubes interact with and respond to viruses in suspension. We exploit the chemical functionalization on nanotubes to tailor the interactions with antiviral antibodies to enable the development of highly selective nanotube sensors for electronic detection of viruses. These devices could find effective use in detection and control of viral diseases, in human and animal populations and in the environment (food, water, and air).

2. Materials and methods

2.1. Device fabrication

The schematic of the overall fabrication process is shown in Fig. 1a. Microfabrication techniques like photolithography, metal etching, and liftoff were used. Chromium (Cr, 100 nm)/gold (Au, 200 nm) was deposited using electron-beam evaporation on a silicon wafer with a 2 μm thick thermally grown silicon dioxide (a and,b). The photoresist (PR) was spun, followed by soft-bake at 105 °C, and exposed to UV (c). After developing, Au and Cr were etched out sequentially as electrodes (d). The photoresist was removed with acetone (e), and a second photolithography was used to fabricate the window area through which SWNTs/polymer layers were assembled on the conducting channel. This would protect the measuring pads for electrical characterization. Layer-by-layer assembly technique was used to assemble SWNTs on the channel. Finally lift-off was used to remove LBL films from measuring pads.

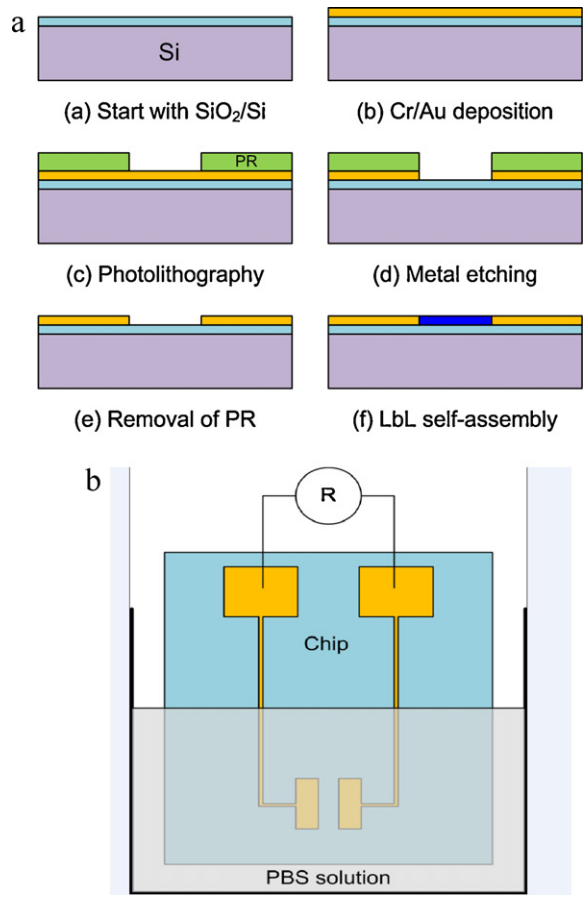

Fig. 1. Schematics of (a) device fabrication and (b) signal testing for device.

2.2. Functionalization of single-walled nanotubes

Chemical functionalization of SWNTs in concentrated acid was performed following previous works [17,18]. The end and side walls of the modified nanotubes are functionalized with carboxylic acids. The FTIR spectrum of functionalized SWNTs displayed a peak at ~1725 cm^{-1}, which corresponds to the C=O stretch mode of carboxylic acid [19].

2.3. Layer-by-layer assembly

The silicon wafer was pretreated with 96% H_2SO_4 and 30% H_2O_2 mixture (3:1 v/v) at 60 °C for 30 min and then rinsed with deionized (DI) water for 10 min. This pretreatment was to remove residuals and contaminations from the surface. To deposit a thin film of polymers using the LBL self-assembly technique, the silicon wafer was immersed into positively charged poly(diallyldimethylammonium chloride) (PDDA) solution (15 g 20 wt% PDDA, 5.8 g NaCl, 200 ml DI water) for 10 min under room temperature. The LBL self-assembly is based on the electrostatic force between two different polymers, one cationic and the other anionic. During the assembly process, the polymer adsorption proceeds until the charge is reversed. In the subsequent step, this is followed by the adsorption of a counter polyion. The alternate adsorption of polyanions and polycations are continued until the desired thickness is achieved. The wafer was then rinsed with DI water on the shaker at 120 rpm for 2 min and air dried and then immersed into negatively charged polystyrene sulfonate (PSS) solution (2 g 30 wt% PSS, 5.8 g NaCl, 200 ml DI water) for 10 min at room temperature. This was followed by rinsing with DI water on the shaker at 120 rpm for 2 min. The polymers were assembled on to the wafer using the LBL technique. The procedure was repeated to deposit an additional layer of PDDA and PSS. In general, SWNTs have low charge density. The initial two layers of PDDA/PSS help anchor the composite to the wafer. This is followed by immersing into PDDA and SWNT solution (0.06 wt%) for 10 min and 15 min, respectively and repeated three times. Between each step, the assembly was rinsed with DI water in the same condition as previously described. This leads to the final device which consists of the original silicon wafer being covered with LBL self-assembled thin film. The final step of the thin film assembly was to deposit a layer of poly(L-lysine) (PLL) on the assembled thin film. The device was immersed into 0.1% PLL solution for 10 min at room temperature. The self-assembled matrix is then cross-linked by immersing in a 0.1% (v/v) glutaraldehyde solution for 2 min. The device was twice rinsed with DI water at 120 rpm for 2 min. The composition of layer by layer assembly was $[(PDDA/PSS)_2 + (PDDA/SWNT)_n]PLL$, where n is the number of SWNT layers.

2.4. Virus propagation and titration

Stock of avian metapneumovirus (aMPV), a pneumovirus of chicken and turkeys, was grown and titrated in Vero cells. The cells were grown in Eagle's MEM supplemented with 10% fetal bovine serum, 150 IU/ml penicillin, 150 μg/ml streptomycin, 50 μg/ml neomycin, 1 μg/ml fungizone, and 5 mg/ml edamin-S. Monolayers of Vero cells were inoculated with aMPV and then incubated

at 37 °C until cytopathic effects were observed, usually within 4 days. The culture was freeze-thawed 3 times followed by centrifugation at 12,000 × *g* for 5 min. The supernatant was aliquoted in 1 ml amounts and stored at −70 °C until used. For virus titration, 100 μl of serial 10-fold dilutions was inoculated in triplicate in Vero monolayers contained in 96-well microtiter plates. After 96 h of incubation, the cells were observed for CPE and 50% tissue culture infective dose ($TCID_{50}$) was calculated by the method of Reed and Muench [20]. The hyperimmune turkey anti-APV serum was produced in isolation reared turkeys and was negative for the presence of extraneous antibodies such as against avian influenza, Newcastle disease virus, and *Bordetella avium* [21]. FITC rabbit anti-chicken/turkey IgG was purchased from Invitrogen (Camarillo, CA) and diluted to 500-fold in PBS.

2.5. Antibody immobilization

The anti-aMPV antibody had a titer of 1:1024 as estimated by an indirect fluorescent antibody test. A 1:300 dilution of the antibody was adsorbed on the PLL coated device by incubating them with known concentration of antibodies in 20 mM PBS buffer (pH 7.4) for a given period of time (12 h) at 4 °C. To prevent non-specific binding we coated the device with the specific antibody followed by blocking all other available adsorption sites with bovine serum albumin (BSA).

2.6. Detection of virus

Suspensions containing stock aMPV were applied to antibody-coated biosensor. The concentration of the virus was varied to estimate the sensitivity of the device. Sensitivity of the device was determined by using various dilutions (1:10, 1:100, 1:500 and 1:1000) of the stock virus (the analyte). Sensing was carried out by monitoring current–voltage characteristics before and after the application of the antigen. A minimum of five devices was tested for each concentration.

2.7. Scanning electron microscopy

For SEM we assembled the exact LBL assembly used for detection on a glass slide. Prior to the assembly, the glass slides were pre-treated with 96% H_2SO_4 and 30% H_2O_2 mixture (3:1 v/v) at 60 °C for 30 min. They were then rinsed with DI water for 10 min. This pre-treatment was to remove residuals and contamination on the glass surface. The treated glass slides became hydrophilic and negatively charged.

After the virus-binding step, glass slides were immersed in 1% (v/v) glutaraldehyde in 0.1 M sodium cacodylate buffer for 10 min to stabilize the viruses and antibodies. The slides were then immersed in a series of increasing ethanol concentrations (v/v) of 50%, 70% and 80% for 5 min each followed by immersion twice into 95% ethanol (v/v) for 5 min. Finally, the slides were immersed into 100% ethanol (v/v) for 5 min and repeated once. At the conclusion of this step, ethanol molecules replaced water molecules in the samples and were ready for the critical point drying procedure. The slides were then transferred to the critical-point dryer in 100% ethanol and dried from liquid CO_2. When completely dried, the slides were sputter-coated it with 2 nm platinum and visualized using SEM (Hitachi S-4700).

2.8. Electrical measurements

The electrical measurement system setup is shown in Fig. 1b. The device was partially dipped in the solution. The multilayer films on top of the conducting channel were immersed in the solution while the elongated electrode pads remained exposed in the air. A voltage (V) was applied on the sensor by attaching two probes to the electrode pads and the current (I) flowing through the channel was measured and recorded. All measurements were conducted in PBS buffer as the baseline fluid at room temperature.

3. Results and discussion

In designing the sensor, two important aspects need to be addressed. The first involves the number of layers of self-assembled components and second is the dimensions of the device. The LBL-assembled devices were tested for their electrical properties. The conductivities depend on charge percolating or the route followed by the current through the randomly distributed conducting filler dispersed in an insulating matrix. The variation of resistance as a function of the number of layers is shown in Fig. 2a. As the number of layers increased, the resistance decreased dramatically and

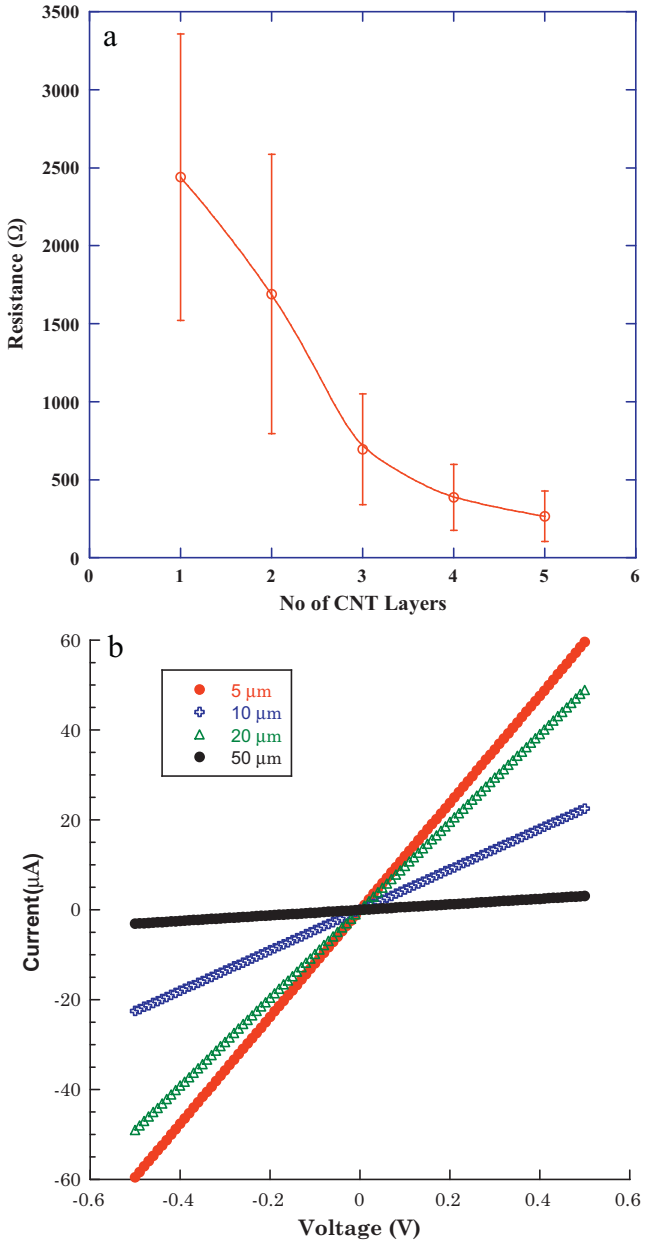

Fig. 2. (a) Resistance as a function of number of deposited SWNT layers (n) in $(PDDA/PSS)_2 + (PDDA/SWNT)_n$. The error bars represent the standard deviation. (b) Current–voltage characteristic of device networks as a function of gap width.

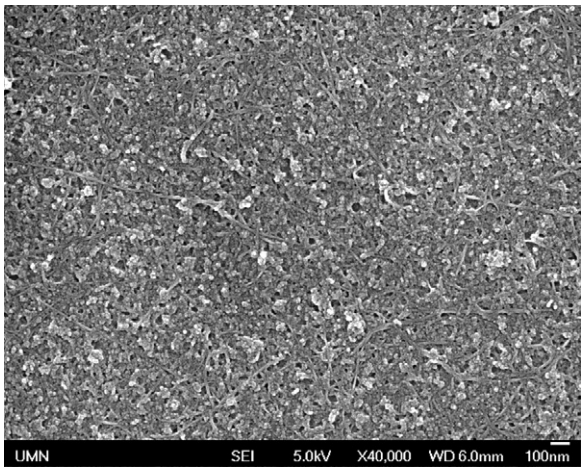

Fig. 3. SEM image for a 5-bilayer PDDA/SWNT LBL film.

plateaued after five layers. This trend is in accordance with that reported in the literature [22–24]. The layered structures are an indication that the CNTs, are predominantly adsorbed parallel to the substrate. The polymers used as the sandwich layer between the two conducting CNT layers are non-conducting, while the CNTs are a third metallic and two-thirds semi-conducting. Hence, the electrical resistance of the composite depends primarily on the resistance associated with the semiconducting and metallic CNT resistances along with the contact resistances of the nanotubes. It has been suggested [22] that the CNT–CNT contact resistance dominate the overall resistance of the composite. When CNTs are deposited on a substrate they typically aggregate into bundles of approximately 50 nm diameter containing a large number of more or less parallel nanotubes [25] which join and intersect with other bundles to form the complete CNT network. The reaching of the plateau value is an indication that the CNT network on the substrate reached the percolation threshold since the randomly oriented CNTs achieved a degree of connectivity.

The variation of conductance as a function of channel width is shown in Fig. 2b. Percolating paths are formed by metallic tubes leading to the ohmic character of the electron transport. This is evidenced from scanning electron microscope image of the 5 bilayer PDDA/SWNT films (Fig. 3). There is no aggregation of the nanotubes and individual nanotubes can be seen to be randomly aligned. The film appears dense but uniform. There are pores evident on the surface. As the channel width increased, the conductance decreased. Reducing the distance between electrodes has been shown to increase electron transfer [26]. For a channel width of 50 μm, which was the largest dimension tested, there was an order of magnitude difference in the value of conductance as the number of layers increased from a single layer to 5 layers. Sensor size affects the total analyte flux. A large capture area is desirable to increase the sensitivity of the device by minimizing the mass transport limitations but would require large amount of nanotubes for covering the area. Hence, in this study, the electrode gap of 20 μm was used.

One of the major challenges in the fabrication of biosensors is to attach antibodies or antigens to the device. In order for a biomolecule to be attached to the device, the charge on the outside layer should be opposite to the charge on the biomolecule. The charge on the anti-aMPV antibody was determined. A negatively charged glass slide was coated with PDDA by dipping into a PDDA solution for 10 min. A second glass slide was coated with PDDA and then a negatively charged PSS. Both slides were immersed in avian serum containing anti-aMPV antibody. The frequency shift in a quartz crystal microbalance (QCM) indicated that the antibody was negatively charged. Using a similar procedure, the antigen was found to be positively charged.

While numerous reports provide evidence that enzymes and proteins can adsorb spontaneously on the sidewalls of acid-oxidized SWNTs [5], there are few reports detailing the adsorption of antibodies on CNTs. The relative size of the virus antibodies (7–10 nm) compared to the diameter of the SWNTs (1–3 nm) may affect the binding and stability of the antibody adsorbed on the CNTs [27]. Hence, it is important to characterize the attachment of antibodies to SWNTs, because the success of the sensor depends on the immobilization of the antibody. We assembled $[(PDDA/PSS)_2 + (PDDA/SWNT)_5]$PDDA on a glass slide. The assembly was then immersed in antibody solution followed by antigen solution with washing steps in between. SEM observations indicated that there were no viruses attached to the surface. A possible reason could be due to the weak binding of the antibody to the device. This would hamper the binding of antigen to these antibodies which could become dislodged during the washing steps.

We then attempted to immobilize the antibody by coating the outer layer with positively charged poly(L-lysine) (PLL) which has been shown to enhance binding of antibodies [28–30]. PLL is a charge enhancer and has plenty of active amino groups. In a preliminary study we verified that coating the surface of the device by PLL does attach the antibody to the device. Since it is difficult to detect antibodies under SEM because of its size, we wanted to ensure that we could successfully immobilize antibody and that virus could be attached to antibody by means of immuno-binding, a technique which was utilized in the electric detection. Negatively charged glass slides were coated with PLL by immersing into PLL solution for 10 min and rinsing by DI water for 2 min, followed by baking at 60 °C. These glass slides were then immersed into 1:300 dilution of turkey IgG solution for 12 h at 4 °C, while a control glass slide was immersed in to 1× PBS. Next, all glass slides including the control slide, were dipped into 1:500 dilution of anti-turkey IgG-FITC solution for 1 h at room temperature. Between each step, the glass slides were washed with 1× PBS (2 min at 120 rpm, repeated once). The immobilization of turkey IgG on the PLL-coated glass slide is shown in Fig. 4a. The control (immersed in PBS) is shown in Fig. 4b. It can be seen that the secondary antibody (anti-turkey-IgG-FITC) bound specifically to turkey IgG.

The aMPV detection was based on the sandwich technique. The primary antibodies (anti-aMPV antibodies prepared in turkeys) were immobilized on glass slides followed by soaking in 1% BSA for 30 min to block all available sites. The slides were then immersed into the stock solution of aMPV suspension followed by the application of 1:300 dilution of anti-turkey-IgG, which was detected by fluorescent-labeled anti-turkey IgG-FITC. Between each step, the glass slides were washed with PBS. The schematic of the sandwich model on a glass slide, where the red circle indicates the aMPV captured by the immobilized turkey IgG is shown in Fig. 4c. When applied with another set of Turkey IgG, the antibody molecules could recognize the virus and form the "sandwich". This sandwich could be detected by anti turkey-IgG-FITC as shown in Fig. 4d. In the control sample, there was no anti-aMPV present (Fig. 4e) so the "sandwich" model could not form, thus there was no binding site for the secondary antibody to recognize. As a result, there was no fluorescence in the control sample.

Next the procedure was repeated using LBL assembly $[(PDDA/PSS)_2 + (PDDA/SWNT)_5 + PLL]$ on a glass side. The entire assembly was cross-linked by immersing in glutaraldehyde solution. Then these glass slides were immersed into a stock solution of 1:300 dilution of turkey IgG solution for 12 h at 4 °C, while a control glass slide was immersed in to 1× PBS. All glass slides including the

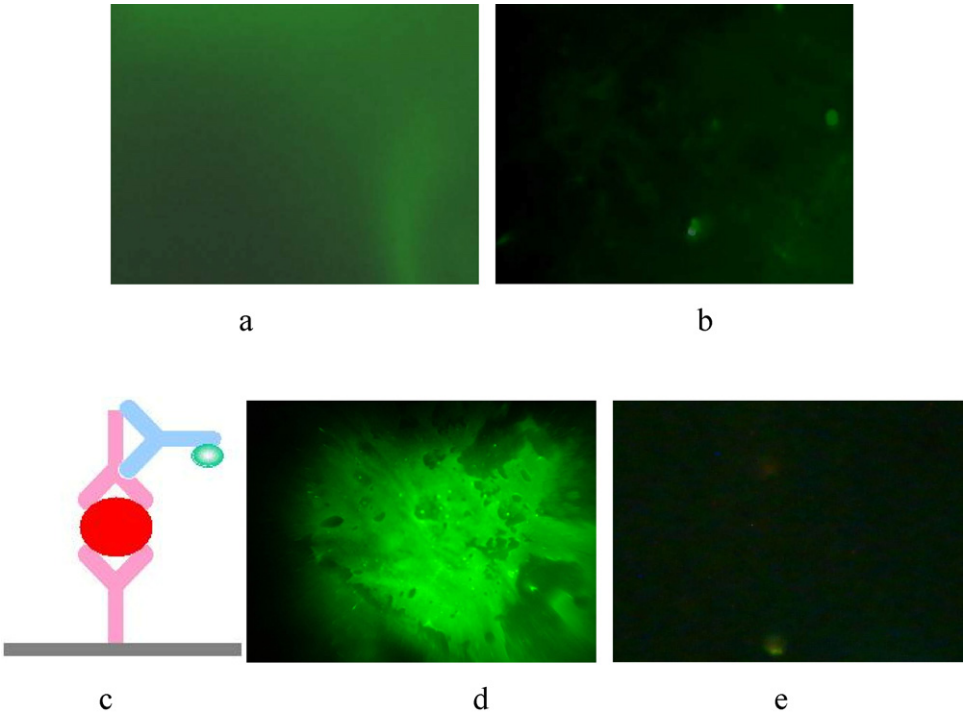

Fig. 4. The immobilized turkey IgG on the PLL-coated glass slide (a) anti-turkey IgG-FITC, and the control (b) without turkey IgG. The aMPV capturing by using the sandwich model, (c) is the schematic of sandwich, anti turkey-IgG-FITC (d) and the control (e) which was immersed in 1× PBS instead of aMPV solution.

control slide, were dipped into 1:500 anti-turkey IgG-FITC solution for 1 h, under room temperature. It is seen in Fig. 5 that the antibody immobilization and virus capturing scheme were working on the thin film. The fluorescent image (Fig. 5a) showed that after immobilization on the thin film surface, the turkey IgG still had the ability to recognize and capture aMPV from the solution. In the sample, there were no virus particles on the surface. There were some fluorescent residues in the picture of the control sample (Fig. 5b). This is attributed to the surface roughness of the thin film. Since the surface was not flat, it would be difficult to wash all the unattached fluorescent-labeled secondary antibodies off the surface.

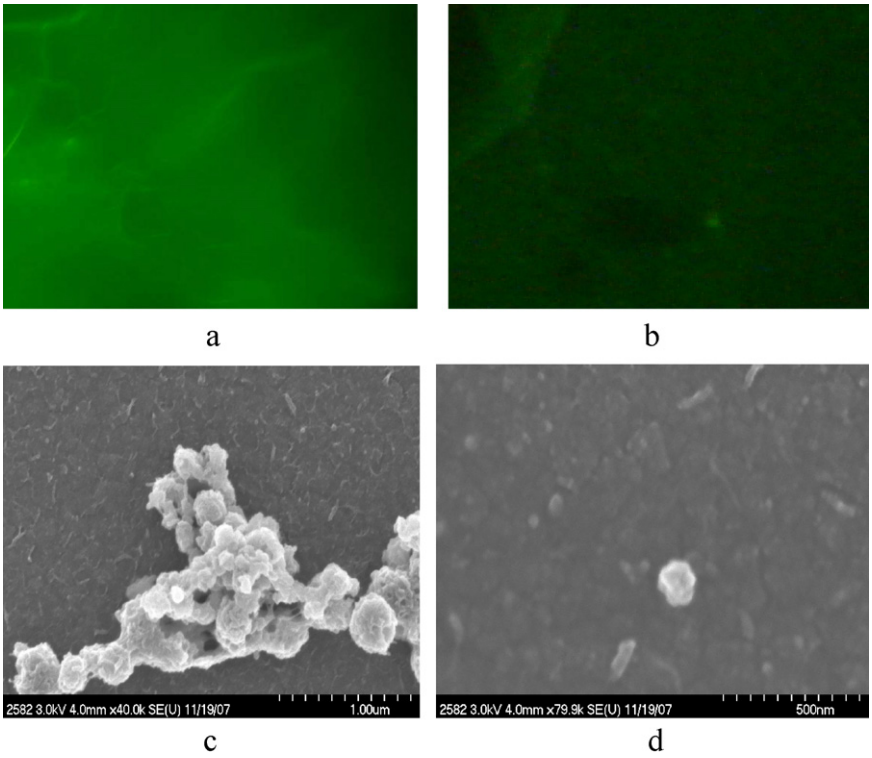

Fig. 5. The sandwich test on thin film with SWNT–PLL covalently attached (a) and control sample (b). SEM pictures on thin film (c and d).

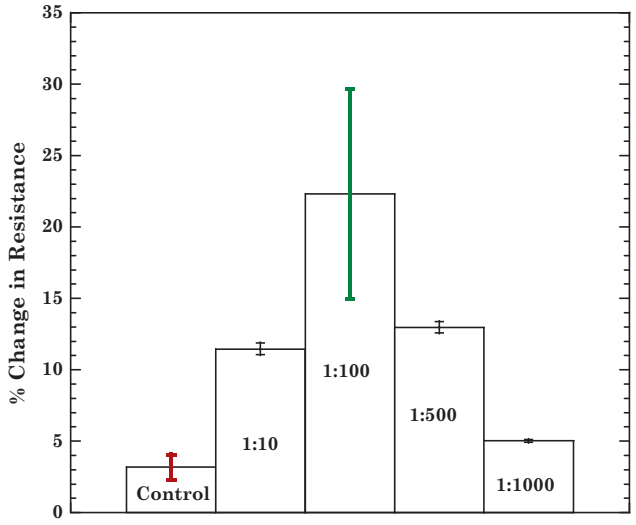

Fig. 6. Average resistance shift versus concentration of antigen for a given antibody concentration. The error bars represent standard deviation.

We also took some SEM pictures of the sample. After immersing into aMPV solution and washing with 1× PBS, we fixed the sample with 1% glutaraldehyde in 0.1 M cacodylate buffer. The samples were dried by critical-point dry technique to prevent virus swelling. The SEM pictures show that aMPV particles were captured by the antibodies that were distributed on the glass surface (Fig. 5c). A closer picture of an individual virus sitting in the center of the field is shown (Fig. 5d). The diameter of the virus is approximately 100 nm. This procedure was fairly reproducible.

When the same procedure (LBL assembly, antibody attachment, antigen capture) was attempted for an assembly that was not cross-linked using glutaraldehyde, the reproducibility was poor. The glutaraldehyde can react with both the amine groups on lysine and the acid groups on SWNT. The cross-linking of the device enhances stability of the structure.

The devices built using LBL assembly $[(PDDA/PSS)_2 + (PDDA/SWNT)_5 + PLL]$ and cross-linked using glutaraldehyde were exposed to solutions containing antibodies and then in PBS solution containing different concentrations of antigen. Measurements were conducted before and after the incubation of the antibody on the sensor. After immobilization of the antibody, the device was incubated in BSA solution for about 1 h in order to block possible active sites to avoid non-specific adsorption. Addition of antigen reduced the conductance. This is in agreement with data presented in the literature [31,32]. The decrease in conductance is due to the electron-donating property of the functional groups of antibodies [33]. However, it has been observed [31,34] that conductance decreased regardless of the sign of the net charge on the biomolecules. Characterization revealed that electronic effects at the metal–nanotube contact due to protein adsorption contribute to the biosensing signal [32]. The antibody and antibody–antigen molecules serve as a barrier against conduction by interfering with electron transfer between electrodes [35].

As a control, experiments were conducted on devices with no antibody attached. The variation of resistance change with concentration is shown in Fig. 6. The antibody was diluted 1:300 (original titer of 1:1024 by indirect fluorescent antibody test). The sensor devices were immersed in the diluted antibody solution for 24 h. These devices were then removed, washed under DI water, and dried under nitrogen. This is followed by immersion in 1 wt% BSA solution at room temperature for 30 min to block the empty sites. The resistance of the antibody-coated device was measured in PBS solution. Finally, the devices were immersed in solution containing the antigens diluted to the required concentration. The devices were left in the antigen solution for 2 h, removed, washed under DI water, and dried under nitrogen. The resistance of the antigen–antibody complexed device was measured while immersed in PBS solution.

The percent change in resistance was calculated as:

$$\frac{\text{resistance with antibody and antigen} - \text{resistance with antibody}}{\text{resistance with antibody}} \times 100$$

As the dilution decreased, the percent change in resistance increased and then decreased. The percent changes in resistance at 1:10 and 1:500 were not significant at 5% confidence level. Results similar to those shown in Fig. 6 were reported by other researchers [36,37]. The minimum detectable concentration is affected by the binding efficiency of antibody to its antigen [38]. As the concentration of antigen increased, there was a competition for the reactive sites on the antibodies – the binding sites may be over crowded by the excess of antigens. The number of antibody molecules immobilized on the sensor device governs the number of active sites available for interaction with antigen. This leads to a hindrance and therefore, reduces the signal intensity. Another problem that affects the sensitivity of these devices is that CNTs are a mixture with predetermined conductive and semi-conductive properties. It is not yet possible to control the electronic property of CNTs during the growth stage. The effective separation of conductive and semi-conductive CNTs from their mixture is still a challenge. The composition of this mixture could further affect the sensitivity of the device.

In our device, the lowest concentration detected was 100 $TCID_{50}$/ml. This sensitivity is higher than the devices mentioned in the literature. The relatively higher sensitivity can be attributed to the higher antibody loading ability of these devices. Gooding [39] has hypothesized that the number of antibodies, each having a surface area of 5 nm^2, that can attach to a single 20 nm diameter nanowire with 20 μm length is approximately 1200. Hence, in a LBL system with multiple CNTs, the number of immobilized antibody is expected to be large.

It is generally expected that the change in resistance with increase in concentration of an analyte would assume the form of a rectangular hyperbola. It has been reported [36] that for a fixed concentration of antigen immobilized on a device, the shifts in signal increased with increasing concentration of antibody in the solution. There is an optimum concentration of antibody for which this increase in signal strength is observed. When the antibody concentration increased beyond the optimum, the signal strength was found to decrease [36]. The inconsistent data at 10^4 $TCID_{50}$/ml is probably because of the insufficient amount of antibodies present to capture the antigens. Furthermore, the time required for immunocapture was constant and higher concentration of antigens was not reflected in the change of resistance. Hence, mass transport limitations would have to be carefully considered in designing devices. An option would be to direct the analyte molecule towards the detection device via the use of electrostatic field [39]. This data indicate that the device used in this study, at a minimum is capable of detecting viral antigens qualitatively if not quantitatively. Other factors affecting the sensitivity of the device are the sensing area and composition of layers. As the dimension of the device decreased, the time required to capture an analyte of a constant concentration increased [40]. Similarly, for a given device dimension, the time allowed to capture an analyte needs to increase as the concentration of the analyte decreased. If there are fewer molecules of analyte in a sample, the time required to reach

the sensing surface would increase. The detection time increases further when high molecular weight proteins such as antibodies are involved [41].

4. Conclusions

This study demonstrates the successful application of a carbon nanotube based sensor developed using a LBL assembly for sensitive detection of viruses in solution. The cross-linked assembly produced a stable film in aqueous condition. The devices with specifically designed surface functionalities can be used to immobilize antibodies. Binding of the antibodies is enhanced by poly(L-lysine). The binding of the viruses to antibodies is reflected in the variation in resistances of the carbon nanotubes in the devices and can be exploited to detect the presence of these viruses in biosensing applications, particularly those requiring early identification. The antibody–antigen interaction was concentration dependent with detection limits of 100 $TCID_{50}$/ml (at the 95% confidence limit) in 2 h. The change in resistance due to antibody–device and antibody–antigen interactions is probably due to the modulation of conductance of the semiconducting nanotubes. The sensitivity and time response are better than most current techniques used for detecting most viruses. The devices are easy to produce, and are reproducible and inexpensive. The parameters affecting the sensitivity of the sensor include the number of layers of CNT and the channel width. Further optimization involving the time of incubation, concentration of antibody, and device dimensions is needed.

References

[1] C. Jianrong, M. Yuqing, H. Nongyue, W. Xiaohua, L. Sijiao, Nanotechnology and biosensors, Biotechnol. Adv. 22 (2004) 505–518.
[2] G. Gruner, Carbon nanotube transistors for biosensing applications, Anal. Bioanal. Chem. 384 (2006) 322–335.
[3] A. Merkoci, M. Pumera, X. Llopis, B. Perez, M. Del Valle, S. Alegret, New materials for electrochemical sensing. VI. Carbon nanotubes, Trends Anal. Chem. 24 (2005) 826–838.
[4] M. Valcarcel, B.M. Simonet, S. Cardenas, B. Suarez, Present and future applications of carbon nanotubes to analytical science, Anal. Bioanal. Chem. 382 (2005) 1783–1790.
[5] E. Katz, I. Willner, Biomolecule-functionalized carbon nanotubes: applications in nanobioelectronics, ChemPhysChem 5 (2004) 1084–1104.
[6] Y. Lin, T. Shelby, H. Li, K.A. Shiral Fernando, L. Qu, W. Wang, L. Gu, B. Zhou, Y.P. Sun, Advances toward bioapplications of carbon nanotubes, J. Mater. Chem. 14 (2004) 527–541.
[7] K. Gong, Y. Yan, M. Zhang, S. Xiong, L. Mao, Electrochemistry and electroanalytical applications of carbon nanotubes: a review, Anal. Sci. 21 (2005) 1383–1393.
[8] P.B. Luppa, L.J. Sokoll, D.W. Chan, Immunosensors – principles and applications to clinical chemistry, Clin. Chim. Acta 314 (2001) 1–26.
[9] S.R. Nettikadan, J.C. Johnson, S.G. Vengasandra, J. Muys, E. Henderson, ViriChip: a solid phase assay for detection and identification of viruses by atomic force microscopy, Nanotechnology 15 (2004) 383–389.
[10] Y.G. Kuznetsov, A.J. Malkin, R.W. Lucas, M. Plomp, A. McPherson, Imaging viruses by atomic force microscopy, J. Gen. Virol. 82 (2001) 2025–2034.
[11] T. Dastagir, E.S. Forzani, R. Zhang, I. Amlani, L.A. Nagahara, R. Tsui, N. Tao, Electrical detection of hepatitis C virus RNA on single wall carbon nanotube-field effect transistor, Analyst 132 (2007) 738–740.
[12] F. Patolsky, G. Zheng, O. hayden, M. Lakadamyali, X. Zhuang, C.M. Lieber, Electrical detection of single viruses, Proc. Natl. Acad. Sci. U. S. A. 101 (2004) 14017–14022.
[13] F. Patolsky, G. Zheng, C.M. Lieber, Nanowire-based biosensors, Anal. Chem. 78 (2006) 4261–4269.
[14] F. Patolsky, G. Zheng, C.M. Lieber, Fabrication of silicon nanowire devices for ultrasensitive, label-free, real-time detection of biological and chemical species, Nat. Prot. 1 (2006) 1711–1723.
[15] A. Ymeti, J. Greve, P.V. Lambeck, T. Wink, S.W.F.M. van Hovell, T.A.M. Beumer, R.R. Wijn, R.G. Heideman, V. Subramaniam, J.S. Kanger, Fast, ultrasensitive virus detection using a Young interferometer sensor, Nano Lett. 7 (2007) 394–397.
[16] A. Ymeti, V. Subramanian, T.A.M. Buemer, J.S. Kanger, An ultrasensitive Young interferometer handheld sensor for rapid virus detection, Expert Rev. Med. Device 4 (2007) 447–454.
[17] D. Lee, T. Cui, Layer-by-layer self-assembled single-walled carbon nanotubes based ion-sensitive conductometric glucose biosensors, IEEE Sens. J. 9 (2009) 449–456.
[18] D. Lee, T. Cui, pH-dependent conductance behaviors of layer-by-layer self-assembled carboxylated carbon nanotubes multilayer thin-film sensors, J. Vac. Sci. Technol. B 27 (2009) 842–848.
[19] M.A. Hamon, H. Hui, P. Bhowmick, H.M.E. Itkis, R.C. Haddon, Ester-functionalized soluble single-walled carbon nanotubes, Appl. Phys. A 74 (2002) 333–338.
[20] L.J. Reed, H. Muench, Simple method for estimating fifty percent end points, Am. J. Hyg. 27 (1938) 493–497.
[21] F.F. Jirjis, S.L. Noll, D.A. Halvorson, K.V. Nagaraja, D.P. Shaw, Pathogenesis of avian pneumovirus infection in turkeys, Vet. Pathol. 39 (2002) 300–310.
[22] B.S. Shim, Z. Tang, M.P. Morabito, A. Agarwal, H. Hong, N.A. Kotov, Integration of conductivity, transparency, and mechanical strength into highly homogeneous layer-by-layer composites of single-walled carbon nanotubes for optoelectronics, Chem. Mater. 19 (2007) 5467–5474.
[23] B.S. Kim, K.D. Suh, B. Kim, Electrical properties of composite films using carbon nanotube/polyelectrolyte self-assembled particles, Macromol. Res. 16 (2008) 76–80.
[24] H.Y. Park, J. Kim, J.Y. Chang, P. Theato, Preparation of transparent conductive multilayered films using active pentafluorophenyl ester modified multiwalled carbon nanotubes, Langmuir 24 (2008) 10467–10473.
[25] A.B. Kaiser, V. Skakalova, S. Roth, Modeling conduction in carbon nanotube networks with different thickness, chemical treatment and irradiation, Physica E 40 (2008) 2311.
[26] Z. Muhammad-Tahir, E.C. Alocilja, Fabrication of a disposable biosensor for *Escherichia coli* O157:H7 detection, IEEE Sens. J. 3 (2003) 345–351.
[27] N.W.S. Kam, H. Dai, Carbon nanotubes as intracellular protein transporters: generality and biological functionality, J. Am. Chem. Soc. 127 (2005) 6021–6026.
[28] N.N. Naguib, Y.M. Mueller, P.M. Bojczuk, M.P. Rossi, P.D. Katsikis, Y. Gogotsi, Effect of carbon nanofiber structure on the binding of antibodies, Nanotechnology 16 (2005) 567–571.
[29] M. Abbasi, H. Uludağ, V. Incani, C. Olson, X. Lin, B.A. Clements, D. Rutkowski, A. Ghahary, M. Weinfeld, Palmitic acid-modified poly-L-lysine for non-viral delivery of plasmid DNA to skin fibroblasts, Biomacromolecules 8 (2007) 1059–1063.
[30] L. Wang, L. Lei, X.F. Ni, J. Shi, Y. Chen, Patterning bio-molecules for cell attachment at single cell levels in PDMS microfluidic chips, Microelectronic Engineering, 86(4–6) MNE'08 – The 34th International Conference on Micro- and Nano-Engineering (MNE), April–June 2009, 1462–1464, ISSN 0167-9317, doi:10.1016/j.mee.2009.01.030.
[31] R.J. Chen, S. Bangsaruntip, K.A. Drouvalakis, N.W.S. Kam, M. Shim, Y. Li, W. Kim, P.J. Utz, H. Dai, Noncovalent functionalization of carbon nanotubes for highly specific electronic biosensors, Proc. Natl. Acad. Sci. U. S. A. 100 (2003) 4984–4989.
[32] R.J. Chen, H.C. Choi, S. Bangsaruntip, E. Yenilmez, X. Tang, Q. Wang, Y.L. Chang, H. Dai, An investigation of the mechanisms of electronic sensing of protein adsorption on carbon nanotube devices, J. Am. Chem. Soc. 126 (2004) 1563–1568.
[33] K. Bradley, M. Brinman, A. Star, G. Guner, Charge transfer from adsorbed proteins, Nano Lett. 4 (2004) 253–256.
[34] K. Teker, E. Wickstrom, B. Panchapakesan, Biomolecular tuning of electronic transport properties of carbon nanotubes via antibody functionalization, IEEE Sens. J. 6 (2006) 1422–1428.
[35] G. Cavelier, Possible role of surface electrochemical electron-transfer and semiconductor charge transport processes in ion channel function, Bioelectron. Bioeng. 40 (1995) 197–213.
[36] Y. Sun, X. Liu, D. Song, Y. Tian, S. Bi, S. Zhang, Sensitivity enhancement of surface plasmon resonance immunosensing by antibody–antigen coupling, Sens. Actuators B 122 (2007) 469–474.
[37] Z. Muhammad-Tahir, E.C. Alocilja, A conductometric biosensor for biosecurity, Biosens. Bioelectron. 18 (2003) 813–819.
[38] J. Xu, D. Suarez, D.S. Gottfried, Detection of avian influenza virus using an interferometric biosensor, Anal. Bioanal. Chem. 389 (2007) 1193–1196.
[39] J.J. Gooding, Nanoscale biosensors: significant advantages over larger devices? Small 2 (2006) 313–315.
[40] P.E. Sheehan, L.J. Whitman, Detection limits for nanoscale biosensors, Nano Lett. 5 (2005) 803–807.
[41] J.V. Veetil, K. Ye, Development of immunosensors using carbon nanotubes, Biotechnol. Prog. 23 (2007) 517–531.

Biographies

Mrinal Bhattacharya received his PhD from the University of Nebraska, Lincoln. He is currently a professor in the Department of Bioproducts and Biosystems Engineering at the University of Minnesota. His research interests are in the use of carbon nanotubes in sensors and tissue engineering.

Shu Hong received his undergraduate degree from Zhejiang University in the Peoples Republic of China in 2006. He is currently pursuing his graduate studies at the University of Minnesota.

DongJin Lee received his PhD degree from the University of Minnesota in 2010. His main research topics include micro/nano manufacturing, nanomaterial based sensors and actuators, chemical and biological sensors, micro- and nanoelectromechanical systems (M/NEMS), and general nanotechnology.

Tianhong Cui received his PhD degree from the Chinese Academy of Sciences, Beijing, China, in 1995. He is currently a Nelson Associate Professor of mechanical engineering at the University of Minnesota. From 1999 to 2003, he was an assistant professor of electrical engineering at Louisiana Technical University. His current research interests include MEMS/NEMS, nanotechnology, and polymer electronics.

Sagar M. Goyal received his PhD degree from the Haryana Agricultural University in India. He is currently a professor of veterinary population medicine at the University. His research interests are in development of rapid methods for the detection of viral infections in livestock and poultry.